JOURNAL OF FIRE SCIENCES

Original Research Article

Journal of Fire Sciences
2024, Vol. 42(4) 314–339

DOI: 10.1177/07349041231210490
journals.sagepub.com/home/jfs
Sage

Improvement of heat release methodologies using mass loss calorimeter and oxygen consumption hood to assess flammability of wood plastic composites

Mark A Dietenberger, Charles R Boardman and Nicole Stark

Date received: 28 July 2023; accepted: 11 October 2023

Abstract

The mass loss calorimeter provides a robust method for evaluating flammability of very sooty materials such as wood plastic composites as a lower cost and rugged alternative to the reliable and effective cone calorimeter. The high amounts of smoke and carbon monoxide associated with these materials resulted in a much-reduced heat release rate, resulting in incomplete combustion of the diffusion flame, which required modifications to the standards in measuring heat release rate via oxygen consumption or carbon dioxide production or thermopiles. In addition to liquid fuels of ethylene glycol and methanol, the solids polystyrene and polymethyl methacrylate were used as calibration materials for the mass loss calorimeter and the instrumented heat release rate hood. Because of concerns about the flue gas thermopile methodology for heat release rate measurements, a second thermopile was attached to the exterior of the metal pipe chimney typically used for heat release rate calculations in the mass loss calorimeter. A heat balance analysis indicated that this is an effective design compared with alternative designs. Estimates of flaming heat release rate are reported using both signals from the thermopiles for calculation of heat release rates and confirmed with the updated oxygen consumption analysis under an instrumented hood. This special fire test arrangement was used to assess the flammability of four different wood

USDA Forest Service, Forest Products Laboratory, Madison, WI, USA

Corresponding author:
Mark A Dietenberger, USDA Forest Service, Forest Products Laboratory, One Gifford Pinchot Dr., Madison, WI 53726, USA.
Email: mark.a.dietenberger@usda.gov

plastic composites, some with fire-retardant treatments, such as ammonium polyphosphate and brominated, all of which tended to have high smoke production leading to high-radiant energy losses. The reduction of heat release rate with 10% by content of fire-retardant treatment was confirmed by both heat release rate measures. The average heat release rate decreased 19% to 39% when fire retardants were added, relative to this wood flour–polyethylene composite.

Keywords
Fire-retardant treatment, heat release rate calorimetry, mass loss calorimetry, wood plastic composite

Introduction

Overview

Wood plastic composites (WPC) present challenges to all testing methodologies designed to measure heat release rate (HRR), including those based on sensible heat, oxygen consumption, and carbon dioxide production. None of the current standard methods provide a correction to the HRR determination for the large soot emission expected for materials, such as polystyrene (PS) and WPC. Although various HRR corrections have been proposed and partly verified (Dietenberger and Boardman,[1] Dietenberger,[2] Brohez et al.,[3] and Lonnermark and Babrauskas)[4] for incomplete combustion, this work presents a more systematic evaluation of HRR methodology to suggest amendments to the standard procedures and provide an updated HRR calculation that can be generally applied to mixed materials or composites.

There is too much error in the heat of combustion (HOC) for standard reference homogeneous materials that do not char. While the stoichiometric net HOC is in relatively close agreement between well-known sources (Babrauskas,[5] Tewarson),[6] the chemical HOC (the HOC due to incomplete combustion) and convective HOC (the HOC to raise the entrained ambient air temperature to the fire exhaust temperature) are basically a single-source tabulation (Tewarson),[6] which for some materials, including a few reference materials, will need to be modified as explained in this article. From here on, we will use "flaming HOC" instead of "chemical HOC" or "effective HOC" to reflect the importance of the diffusion flame in affecting incomplete combustion and to distinguish the HRR methodology proposed here. The flaming HOC is always somewhat less than the net stoichiometric HOC because all diffusion flames have some amount of inefficient combustion in the form of carbon monoxide and soot emissions.

The soot and carbon monoxide emissions (as mass fractions of volatilized fuel mass) generally do not scale with the size of fire in the case of woody materials in the same way as the hydrocarbon fires (Dietenberger et al.),[7] so the flaming HOC varies with the size and level of confinement of the fire for such materials. The flaming HOC needs to be measured for the various reference materials for a given HRR apparatus rather than obtained from those tabulated with a different apparatus, which may use a less accurate HRR methodology, or has a different scaling effect on soot and carbon monoxide. By multiplying such an improved flaming HOC by the mass loss rate (MLR), one will obtain a suitably accurate flaming HRR. For this work, the mass loss calorimeter (MLC), see Figure 1, was placed under a mid-sized HRR-instrumented "room-burn" hood (ie. ISO9705), which used oxygen

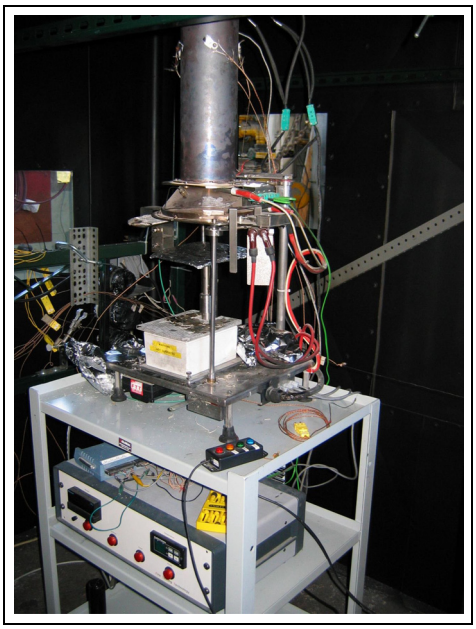

Figure 1. Modified MLC under Forest Products Laboratory's (FPL's) HRR hood surrounded by radiant absorbing walls.

consumption for HRR calculation. This combination was calibrated with several reference materials, offering an opportunity to revisit all the HRR methodologies and thus provide a unified HRR measurement for the WPCs examined. The primary focus in this work is to show improvements in accuracy for the MLC, especially at the low HRR levels typical of WPC which use fire-retardant additives.

Concerning previous improvements to HRR instruments

To improve the measurement of HRR, the MLC was modified previously to include a thermopile on the exhaust pipe stack, that is, the chimney, (in addition to the thermopile in the flue gas exhaust) as shown in Figure 1. This better accounts for the convective and radiant energy losses to the chimney wall (Dietenberger and Boardman).[1] The wall thermopile was placed at mid-height in the stack, and its temperature signal is combined with the flue gas temperature as subsequently described to measure the HRR. The rest of the MLC is standard with a spark plug pilot igniter and a truncated conical electric heater that provides a constant heat flux of up to 100 kW/m^2 onto a test specimen of up to 50 mm thick. Furthermore, a set of reference calibration materials was used that produced both high and low radiant transfer to the walls. So, instead of only the standard methane, both pure ethylene glycol and methanol were used for low flame radiant losses, while polymethyl methacrylate (PMMA) and solid Rexolite® PS provided high flame radiant losses because of the sooty smoke produced. As previously introduced and discussed later, the flaming HOC for these proposed reference materials was updated for this calibration. Mass loss data were

processed using a Savitzky–Golay (SG) digital filter followed by an exponential low-pass filter so that the mass loss profile as multiplied by flaming HOC of reference materials was synchronized with the HRR profile of either the sensible HRR or that of HRR via oxygen consumption. Finally, for this study, alternative sensible HRR designs were evaluated for measuring the enthalpy heat rise of the flue gas and the corresponding convective and radiative heat losses to the firebox and chimney walls for determining the flaming HRR (Moussan et al.,[8] Filipczak and Lyon,[9] Anderson,[10] Quintiere et al.,[11] ASTM E1321 (LIFT apparatus),[12] and ASTM E906.[13]). It will be shown using heat balance analysis and the use of four reference materials that the current low-cost MLC design[14] (ASTM E2102-15) is effective and that added features such as anemometers, oxygen sensors, differential pressure probes, chimney insulation, and water jacketing will not be necessary, nor advisable.

The described MLC was positioned under the Forest Products Laboratory's (FPL's) HRR hood, which uses oxygen consumption to calculate HRR (Dietenberger and colleagues).[15] The burn room was closed off. The HRR hood's exhaust pipe is instrumented with a bidirectional velocity probe, a pair of thermocouples, red laser smoke extinction, and extraction for gas analysis of O_2, CO_2, CO, and H_2O with time. The exhaust blower was outfitted with an electronic control system to lower the exhaust flow much below the standard 1 m^3/s to increase the accuracy of the low flaming HRR values. The updated instrumentation and data acquisition analysis provided the ability to determine the stoichiometric, flaming, and convective HRR components of a flaming fire for a wide range of HRR values, as will be evident in this article. A completely walled-in hood, except for the north side doorway, with high-emissivity paint coating helps achieve better accuracy in the radiant fraction measurements. Indeed, the convective HRR as divided by the MLR for reference materials in open flames was found comparable with the convective HOC values listed by Tewarson.[6] Further details on the accuracy of the FPL's HRR hood are provided in a later section.

Concerning inadequate calibration procedures

As introduced, to improve HRR accuracy of the MLC for WPC (Stark et al.[16]), three new reference materials, ethylene glycol, PMMA, and PS, were tested in addition to the standard methane. Other standard MLC measured parameters such as the time to ignition and MLR (adjusting for differences in weigh scale response factor) corresponded closely with the cone calorimeter[17] (ASTM E1354) in previous studies (Hasburgh et al.,[18] Dietenberger and Boardman)[1] as would be expected from the similarity of cone heater and cone holder design. Discrepancies of the HRR based on the thermopile data with the HRR based on oxygen consumption were shown to be reduced with the introduction of a chimney thermopile (Dietenberger and Boardman),[1] but this addition should be further reviewed with heat balance and uncertainty analyses and examination of alternative sensible HRR designs. Some continuing problems were noted, such as whether the flue gas thermopile was clean or dirty, inadequate accounting for radiant heat losses, and defining the zero level HRR, particularly during the cool-down phase of the chimney when fire extinction occurred (Hasburgh et al.).[18] Because of these issues, it was not clear if the chimney thermopile would be useful for fire-retardant treated (FRT) wood products, which have quite low HRR, as do the FRT WPC used in this study. All these issues were addressed in the revised MLC methodology for HRR.

Furthermore, additional calibration issues exist outside the issues with using MLC for HRR. Introducing the PS with its high smoke production can lead to the error of the HRR

based on O_2 consumption or HRR based on CO_2 production via the standard[19] (ASTM E2058-13a). Here we review standard procedures for HRR determination and then subsequently discuss these additional issues and methods suggested for improvement. The ASTM E2102-15 standard for the MLR calorimeter correlates the measured burning methane HRR as a linear relation with flue gas thermopile temperature rise

$$Q_{T,std} = C_{methane}\ T_p \quad T_0 \tag{1}$$

The subscript std refers to the standard method, T_p is the plume temperature at the top of the chimney, and T_0 is the room temperature. Because the mass flow rate of methane is measured as distinct steps, it was digitally filtered with a low-pass filter to match the time response of the thermopile. Multiplying this filtered mass flow rate of methane by its stoichiometric net HOC (as lower heating value (LHV) of 50 kJ/g in Table 1 for methane) provided the calibrating HRR as

$$Q_{M,std} = \dot{m}_f HOC_{Stoich} \equiv \dot{m}_f \Delta h_{f,net} \tag{2}$$

The net HRR provided in the standards (e.g. ASTM E1354) has the net heat release correlated with the oxygen mass consumption rate as

$$Q_{O2,std} = 13.1\ \Delta \dot{m}_{O2} \tag{3}$$

Although the value 13.1 kJ/g, as net heat release per oxygen mass consumed, has been accepted in several standards, the standard for the Fire Propagation Apparatus (FPA) (ASTM E2058-13a) uses the value 12.8 kJ/g, a slightly lower value probably biased toward hydrocarbon fuels. This standard (ASTM E2058-13a) provides yet another correlation for the HRR based on carbon dioxide and carbon monoxide production

$$Q_{CO2,std} = 13.3\ \dot{m}_{CO2} + 11.1\ \dot{m}_{CO} \tag{4}$$

The appendices of ASTM E1354, Babrauskas[5] (1992), and Janssens and colleagues[20,21] (1995) provide the formulae and method to calculate the various mass flow rates when gas measurements are provided for oxygen, carbon dioxide, water vapor, and carbon monoxide.

Table 1. Net heat of combustions (HOCs) for six reference fuels and for WPC including handbook values.

Fuel	Net HOC (kJ/g)						
	LHV[1]#1[6]	LHV[1]#2[5]	Stoichiometric (Equation (5))	Chemical[6]	Flaming (Equation (8))	Convect[6]	Flaming - Convect
Methane	50.1	50.03	50.0	49.6	48.7	42.6	6.1
Propane	46.0	46.36	46.0	43.7	45.4	31.2	14.2
Methanol	20.0	19.94	19.8	19.1	19.5	16.1	3.4
Ethylene glycol	18.2[2]	17.05	17.1	17.6[2]	16.6	13.4[2]	3.2
PMMA	25.2	24.88	25.4	23.1	24.8	15.0	9.8
Polystyrene	39.2	39.75	40.7	29.6	31.5	14.0	17.7
WPC	N/A	N/A	19.6	N/A	18.6	N/A	N/A

[1]Lower Heating Value (LHV); [2]Prestone brand, tabulated.

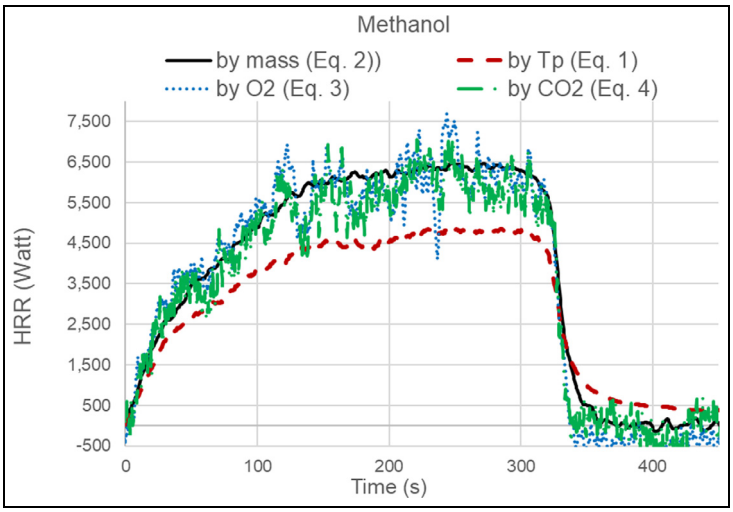

Figure 2. Standard HRR for methanol by four different methods (equations (1)–(4)).

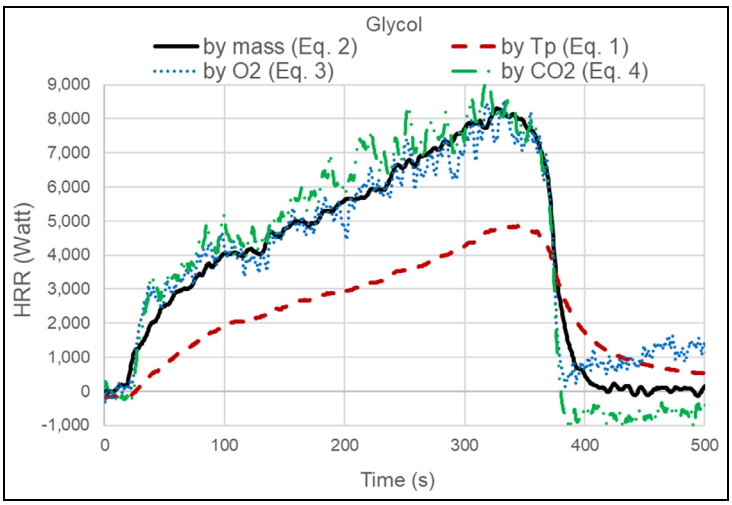

Figure 3. Standard HRR for ethylene glycol by four different methods (equations (1)–(4)).

The "chemical" HOC in Table 1 is the FPA net HRR integrated with time as divided by the fuel mass loss, which they list for the six reference fuels in the SFPE Handbook.[6] However, the flaming HOC in the MLC for the WPCs is derived in a later section.

Figures 2 to 5 show results from the four common HRR calculations (equations (1)–(4)) for the four reference materials (methanol, glycol, PMMA, and PS), under the MLC at 50 kW/m^2 irradiance and the FPL's instrumented hood. The solid black line labeled "by mass (Stoich)" uses equation (2) to calculate the HRR. The dashed line labeled "by temperature (standard)" uses equation (1) as specified with ASTM E2102. The blue dotted line labeled "by O_2 (standard)" uses equation (3), and the combined dashed and dotted line

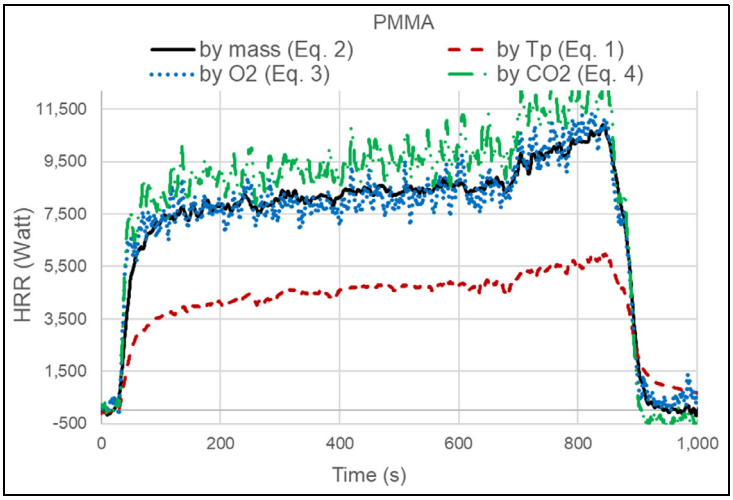

Figure 4. Standard HRR for PMMA by four different methods (equations (1)–(4)).

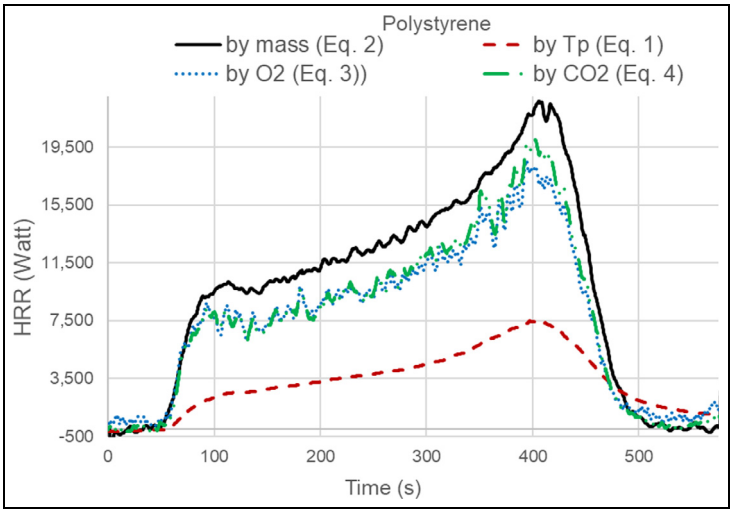

Figure 5. Standard HRR for PS by four different methods (equations (1)–(4)).

labeled "by CO_2 (standard)" uses equation (4). These figures demonstrate that as the material burned in the MLC under the FPL's instrumented hood is moved from methanol to glycol to PMMA to PS, equations (1)–(4) for calculating the HRR increasingly diverge from each other and become inconsistent with each other, with PS being the worst due to its high soot production and associated high radiant heat losses. That is, in the case of PS being a candidate as a reference material that is pure and does not char, has its HRR = MLR × LHV perhaps 33% higher than the oxygen consumption HRR, and worse yet the thermopile HRR by the standard method is one half of the oxygen consumption HRR. The HRR by CO_2 standard differs from the O_2 consumption HRR by up to

13% depending on the fuel. Therefore, adjustments are needed to all forms of HRR determinations as represented by equations (1)–(4) and discussed in the next section.

Flaming HOC and HRR for reference materials in MLC

Background on flaming HRR using CO and soot production

Fortunately, there are published methods that consider the effect of CO and soot production on the reduction of the stoichiometric net HOC (Dietenberger,[2] Brohez et al.,[3] Lonnermark and Babrauskas)[4] that typically occurs in diffusion flames. If the fuel's mass content of carbon, hydrogen, oxygen, nitrogen, sulfur, and ash ($c, h, o, n, s,$ *and* a) is available for direct and premixed combustion with oxygen, then an accurate simple formula for the stoichiometric net HOC (correlation coefficient with r-square of 0.99) is given by Dietenberger[2] for a wide range of fuel, including the hydrocarbons

$$\Delta h_{f,net} = 13.23\ r_o + 9.428\ s \quad (0.9 + 6r_A)\mathrm{H}[r_A \quad 0.17] \equiv \Delta h_{ox,net} r_o \qquad (5)\leftarrow$$

where the stoichiometric oxygen mass consumed to the fuel mass combusted is given by

$$r_o = 8c/3 + 8h \quad o \qquad (6)\leftarrow$$

And the aromatic factor is given by

$$r_A = (h \quad o/8)/c \qquad (7)\leftarrow$$

H is the Heaviside function, which is zero when the independent variable is negative and is unity when the independent variable is positive. Further definitions of the variables are given in the nomenclature section. To obtain the predictions listed in Table 1 under equation (5) column for the stoichiometric HOC, the mass fractions $c, h,$ and o from Table 2 for the reference fuels were used and $n, s,$ *and* a were set to zeroes.

Because CO and soot are the main fuel left over after incomplete combustion of the diffusion flame, it was inferred that the actual flaming HOC is reduced from the stoichiometric

Table 2. Fuel combustion empirical formula and HOCs for reference fuels and WPC.

Fuel: CxHyOz	x	y	z	c Carbon fraction	h Hydrogen fraction	o Oxygen fraction	$\Delta h_{ox,net}$ kJ/g[6]	$\Delta h_{ox,net}$ kJ/g (Equation (5))	$\Delta h_{co2,net}$ kJ/g (Equation (10))
Methane	1	4	0	0.75	0.25	0	12.51	12.51	18.19
Propane	3	8	0	0.818	0.182	0	12.78	12.62	15.29
Ethylene	2	4	0	0.857	0.143	0	13.78	13.23	14.43
Methanol	1	4	1	0.375	0.125	0.5	13.29	13.23	14.43
Ethylene glycol	2	6	2	0.387	0.097	0.516	13.22	13.23	12.03
PMMA	5	8	2	0.6	0.08	0.32	12.97	13.23	11.55
Polystyrene	8	8	0	0.923	0.077	0	13.19	13.23	12.03
Polyethylene	6	12	0	0.857	0.143	0	12.63	13.23	14.43
Cellulose	6	10	5	0.444	0.062	0.494	13.61	13.23	9.62
WPC	6	11.2	4	0.489	0.076	0.435	N/A	13.23	10.90

Table 3. Percentages for various correcting terms for HRR in flaming conditions with MLC tests.

Fuel	% of HOC for CO in equation (8)	% of HOC for Soot in equation (8)	% Difference of equation (12) to equation (3)	% Difference of equation (14) to equation (4)
Methanol	1.38	0.58	0.65	8.97
Ethylene glycol	2.44	0.44	0.38	−9.71
PMMA	1.19	1.27	0.78	−13.03
Polystyrene	2.65	19.58	2.06	−1.38

value by the amount of potential heat that would have been obtained from the combustion of CO and soot, which is given by

$$\Delta h_{f,flaming} = \Delta h_{f,net} \quad (10.1\ \dot{m}_{CO} + 32.8\ \dot{m}_{soot})/\dot{m}_f \tag{8}$$

Other fuels present in the plume gases, such as the primary fuel or its derivatives, are considered negligible as affecting the HOC, and in the case of glycol, our FTIR measurements with the cone calorimeter show these fuels are in the parts per million range compared with the percentage range for H_2O and CO_2 combustion products. The gas analyzers (Sable PA-10 and CO_2/CO NIRs) provided volume concentrations of O_2, CO_2, and CO, whereas the diode laser and sensor in the red wavelength provided the extinction coefficient k_{ext} in the following equation for the soot mass flow rate (Grexa et al.)[15]

$$\dot{m}_{soot} = \frac{k_{ext}}{8.3} \quad (\frac{\dot{m}_{ex}}{\rho_{ex}}) \tag{9}$$

where exhaust mass flow rate and density, $\dot{m}_{ex}$ and ρ_{ex}, are evaluated at the laser line location. Equations (8) and (9) are essentially identical to that described in Brohez et al.[3] after converting from their molar basis to mass basis and setting the specific soot extinction area to 8.3 m^2/kg. However, they did not have access to equation (5) formula for the stoichiometric net HOC. Table 1 lists the flaming net HOC for the six reference materials calculated from equation (8) using the measurement of CO and soot mass flow rate in the HRR hood, fuel mass flow rate calibrated for methane and propane open flame, and MLC measurement of the fuel MLR for methanol, ethylene glycol, PMMA, and PS. Table 3 shows the need for equation (8) for determining the flaming HOC. It is shown that the contribution of the unburned products of CO and soot in the flue gases is very significant for PS and is of some significance for methanol, glycol, and PMMA.

Any discrepancies between the reported values and the FPA measurements (Tewarson)[6] are more likely due to the differences in HOC formulations than to the differences in the diffusion flame environment or differences in calculating the mass flow rates of O_2, CO_2, CO, and soot, as follows. Knowing the fuel empirical formula, it is simple to convert equation (5) from the oxygen consumption basis to the carbon dioxide production basis as in

$$\Delta h_{f,net} = \Delta h_{CO2,net}(44c/12) = \Delta h_{ox,net} r_o \tag{10}$$

If the fuel empirical formula is unknown, there is the availability of equations (3) or (4) to estimate the flaming HRR. However, as was noticed in the introduction with the reference

materials, the presence of high soot amounts can lead to large discrepancies in the HRR estimates. For biomass materials, the sulfur content is negligible and aromatic factor is typically less than 0.17, giving a potential for greater accuracy for the oxygen consumption HRR by an adaptation of equations (5), (8), and (10) as the equations

$$Q_{m,flaming} = \Delta h_{f,flaming} \dot{m}_f \tag{11}$$

$$Q_{O2,flaming} = \Delta h_{ox,net} r_o \dot{m}_f \quad (10.1\ \dot{m}_{CO} + 32.8\ \dot{m}_{soot}) = Q_{m,flaming} \tag{12}$$

Where the estimated stoichiometric oxygen mass consumption rate is slightly higher than the actual oxygen mass consumption by the mass of oxygen needed to combust CO and soot

$$\dot{m}_{O2,stoch} = r_o \dot{m}_f = \Delta \dot{m}_{ox} + \frac{16}{28}\dot{m}_{CO} + \frac{32}{12}\dot{m}_{soot} \tag{13}$$

Because CO and soot productions are commonly measured in the typical HRR facility, it is recommended to implement equations (12) and (13) instead of equation (3) for such facilities. Table 3 shows that, at least for the reference materials used in this study, the percentage error is small when comparing equation (12) to equation (3), with it being as high as 2% for the PS. In this respect, any results with the cone calorimeter for these materials should be comparable with the flaming results from this study with the MLC under the HRR hood. Of course, if the fuel composition is known, then the full equation (5) is recommended. An alternate flaming HRR based on estimating the stochiometric CO_2 production can be obtained with the following equation, with similar estimation

$$Q_{CO2,flaming} = \Delta h_{CO2,net}\ \ \dot{m}_{CO2} + \frac{44}{28}\ \dot{m}_{CO} + \frac{44}{12}\dot{m}_{soot} \qquad (10.1\ \dot{m}_{CO} + 32.8\ \dot{m}_{soot}) \tag{14}$$

These HRR formulations are equivalent to that by Brohez et al.,[3] who used the molar basis rather than the mass basis (previously mentioned), and to Lonnermark and Babrauskas,[4] who provided values already in the mass basis. Another difference is that Brohez et al.[3] used the experimental value for the HOC per stoichiometric mass CO_2 produced, whereas equation (10) is used for this study to derive similar values for the HOC per stoichiometric mass CO_2 produced for whenever the fuel empirical formula is available. Lonnermark and Babrauskas[4] used the well-known heats of formation for their list of fuels and combustion products to arrive at the actual HOC for the incomplete combustion. The fuel empirical formula for the reference materials (methane, propane, ethylene, methanol, ethylene glycol, PMMA, and PS) is provided in Table 2 along with the values for HOCs defined with equation (10) and compared with tabulated values (Babrauskas et al.).[5] Indeed, Lonnermark and Babrauskas[4] listed several fuels in common with those in Table 2, which included methanol and propane. Comparing the coefficient values of equation (14), we note they are within 0.1% and 0.5% for CO_2, 1% and 2% for CO, and 1.4% and 3% for C (soot), respectively, of each other. That is, the final column in Table 2 as derived from equation (10) is in close agreement with the study by Lonnermark and Babrauskas[4] for methanol and propane. The implication is that the coefficient of 13.3 kJ/g in equation (4) is responsible for its ~10% bias with equation (3) as shown in Figures 2 to 5 and summarized in the fourth column in Table 3 for the four reference materials. Surprisingly, the difference between equations (14) and (4) is only 1.4% for PS, given that the PS soot byproduct decreases the net HOC by 20% (see Table 3) in the MLC flames.

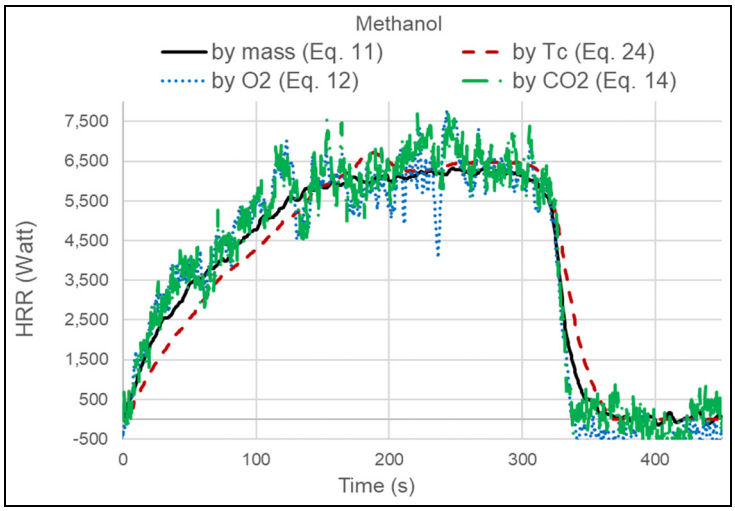

Figure 6. Flaming HRR for methanol by four different methods in close agreement.

There is then an obvious advantage to using equation (14) (or equation (12)) whenever the heats of formation are unavailable among the reactants or when a composite fuel is represented, as would be the case for WPCs. The availability of three different forms of the flaming HRR calculations that are principally equivalent allows one to select the form that gives the most reliable result. This often results in the use of the oxygen consumption equation (12) because of the relative constant value for the HOC per consumed stoichiometric oxygen and a supposed reliable O_2, CO, and soot mass flow rate in the exhaust. The wide-ranging values for the stoichiometric HOC per CO_2 mass production indicate that it would be more beneficial to have the fuel empirical formula available in the case where the most reliable values are CO_2, CO, and soot mass flow rates, for example, when poor O_2 measurement results from aberrations or is inadvertently turned off. This indeed has happened in some of the MLC measurements of WPC combustion under the HRR hood. The requirement for the empirical formula of the WPC to evaluate the flaming HRR based on equations (14) and (10) is addressed in a later section.

Flaming HRR and HOC calibrations particular to MLC test

As seen in Figures 6 to 9, good agreement is now obtained with the three different forms of flaming HRR for the four reference materials. In each figure, the solid black curves are calculated with equation (11) (as $Q_{m,flaming} = \Delta h_{f,flaming}\dot{m}_f$), the blue solid circle points are calculated with equation (12) (as oxygen consumption HRR with soot and CO adjustments), and the green dash–dot curves are calculated with equation (14) (as CO_2 production-based HRR with soot and CO adjustments), all showing close agreement, perhaps within 10% random error, compared with various bias errors in Figures 2 to 5, and in particular, the 50% bias error shown in Figure 5 for the PS material. The Rexolite® PS is then reaffirmed as a feasible reference material with a constant value of flaming HOC as being independent of HRR levels and history, although other similar PS are available. These results provide a reliable flaming HRR as a basis for the calibration of the thermopile-based flaming HRR. The dashed "by

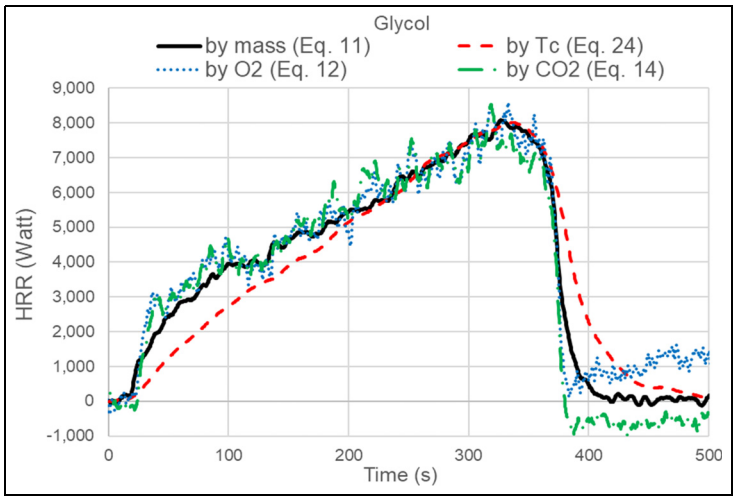

Figure 7. Flaming HRR for ethylene glycol by four different methods in close agreement and comparison with cone calorimeter of a similar glycol mass content.

Tc" line in these figures will be subsequently discussed. It is noteworthy that the flaming HOC (equation (8)) for all the reference materials differs somewhat from that measured with FPA and is considered more representative of the cone calorimeter diffusion flame geometry and therefore provides the more accurate estimates listed in Table 1.

Verification of the instrumented hood, MLC, and material calibrations

The modification to the room-burn standard for the low HRR applications, even the HRR as low as the FRT WPC, included using the well-known calibration of the bidirectional probe as a function of Reynolds number, proper low-pass digital filtering of the probe's differential pressure signal, and higher accuracy gas analyzers beyond that required in the standard. In addition to weighing the propane mass loss as multiplied by its HOC, for calibrating the "C-factor," we also used methane and methanol mass losses during flaming with their well-known HOC to verify that the "C-factor" is unchanged for low HRR applications that required much-reduced exhaust flow rate to around 0.1 m^3/s. However, the use of reference materials in the MLC offered another opportunity to recheck the instrumented hood calibration. As a start, Figures 6 to 9 show that the measurements for the fuel MLR of the MLC and the exhaust flow rate of the instrumented hood along with gaseous and soot volume fractions are essentially synchronized. Indeed, whenever the weigh scale is not available, or is in doubt due to the condensed fuel ejecting particles or foaming up against the heater, the MLR can alternatively be based on the stoichiometric CO_2 production using the composition from Table 1 as the equation

$$\dot{m}_{f,CO2} = \frac{12x + y + 16z}{44x} \quad \dot{m}_{CO2} + \frac{44}{28}\,\dot{m}_{CO} + \frac{44}{12}\dot{m}_{soot} \tag{15}$$

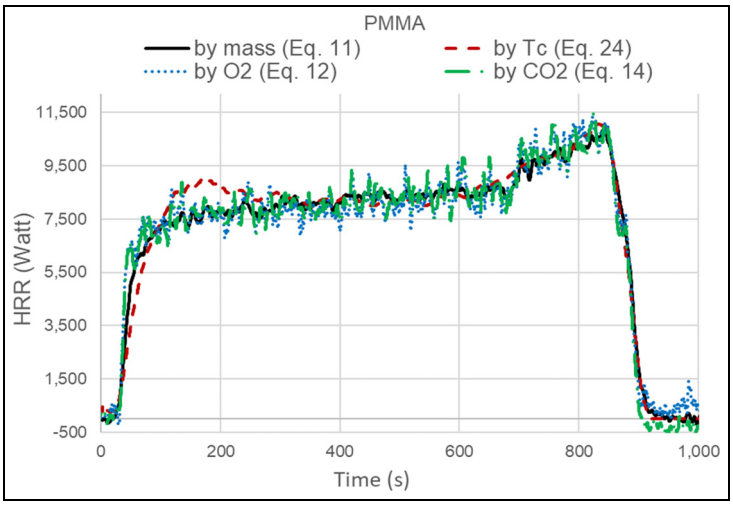

Figure 8. Flaming HRR for PMMA by four different methods in close agreement and comparison with cone calorimeter test with a smaller mass PMMA sample.

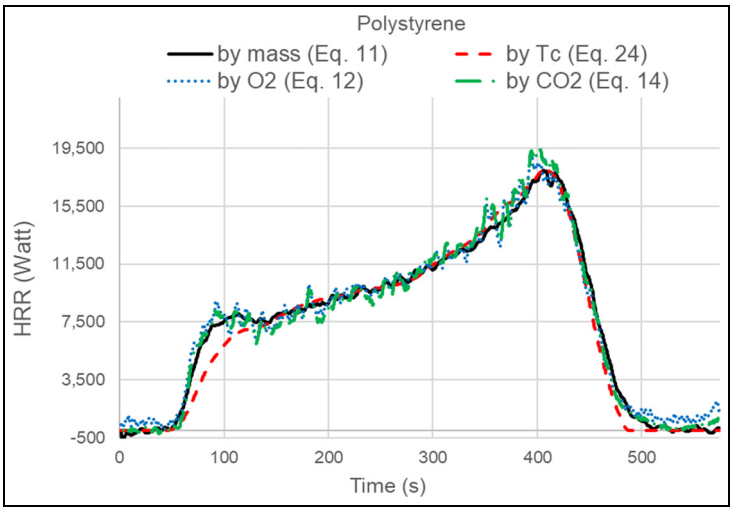

Figure 9. Flaming HRR for PS by four different methods in close agreement.

The overall percentage error in using equation (15) instead of the MLC weight scale–derived MLR in equation (8) for flaming HOC with the four reference fuels is shown in the first column in Table 4. Given the noisiness of the data in Figures 6 to 9 for the four reference fuels, particularly noting that between the black solid lines and the green dash–dot lines, the correlations of between 0.89 and 0.98 for equation (15) to the weigh scale data are noteworthy. Assuring the accuracy of the MLR will then provide the needed flaming HOC, computed as flaming HRR via equations (12) or (14) divided by the MLR for the reference fuel via equation (15), which also agrees with the values in the flaming HOC column in Table 1.

Table 4. Percentage errors concerning mass balance in MLC tests.

Fuel	% error in HOC in using equation (15)	Correlation of equation (15)	% error *c*	% error *h*	% error *o*
Methanol	2.11	0.93	1.61	0.56	−1.34
Ethylene glycol	0.02	0.94	−0.41	−0.38	0.38
PMMA	0.005	0.89	−0.47	−0.41	0.98
Polystyrene	−0.52	0.98	−1.17	−0.18	N/A

This synchronization of the condensed fuel MLR with the mass production rates of combustion products and oxygen consumption will assist in identifying the empirical fuel formula of the WPCs as discussed here. That is, the pure organic fuel volatile mass rate (used in equation (11)) plus the stochiometric oxygen consumption mass flow rate (from equation (13)) minus the stochiometric carbon dioxide mass flow rate (from equation (14)) is set equal to the stochiometric combustion water vapor flow rate to achieve combustion mass balance for a fuel with low sulfur and nitrogen contents, as in

$$\dot{m}_{H2O,\,stoich} = \dot{m}_f + \dot{m}_{O2,\,stoich} \quad \dot{m}_{CO2,\,stoich} \tag{16}$$

The low sulfur and low aromatic value of WPC volatiles indicates that $\Delta h_{ox,\,net} = 13.23\ kJ/g$, so that equation (10) can be used to get agreement among the three different forms of flaming HRR calculations. The fuel volatile then has the derived elemental mass fractions, which add up to unity, as

$$c = \frac{12\ \dot{m}_{CO2,\,stoich}}{44\ \dot{m}_f},\ h = \frac{2\ \dot{m}_{H2O,\,stoich}}{18\ \dot{m}_f},\ o = \frac{32\ \dot{m}_{CO2,\,stoich}}{44\ \dot{m}_f} + \frac{16\ \dot{m}_{H2O,\,stoich}}{18\ \dot{m}_f} \quad \frac{\dot{m}_{O2,\,stoich}}{\dot{m}_f} \tag{17}$$

Application of equation (17) to the reference fuels resulted in the overall percentage errors for their corresponding carbon, hydrogen, and oxygen contents as shown in Table 4. The low percentage errors shown in Table 4 indicate that the HRR facility is very well calibrated for the 0.1 m^3/s exhaust flow rate and for the measurements of the flue composition, including that of the soot. These results place greater confidence when addressing the WPC fuel samples with corresponding low HRR values, which can challenge both MLC and instrumented hood calibrations. Therefore, Table 2 provides the empirical fuel formula as derived with equation (17) for WPC, $C_6H_{11.2}O_4$, but because of its charring nature, the actual WPC empirical formula may be different in the virgin state. Comparison with polyethylene and cellulose as the main constituents of WPC shows the reasonableness of its empirical formula and HOCs listed in Table 2. This WPC composition calibration was particularly important because the CO_2 and CO measurements were more accurate and reliable than the O_2 measurement for some tests of FRT WPC. These tests had very low HRR values challenging the accuracy limits of the HRR hood and the MLC thermopile measurements, for which comparison with the cone calorimeter HRR measurements of similar WPCs was beneficial in verifying or even adjusting the thermopile HRR calibration, as will be subsequently shown.

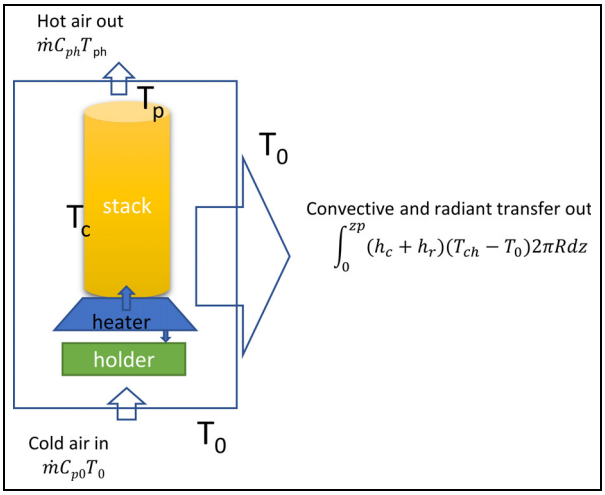

Figure 10. Control volume schematic of MLC describing the heat balances using physical boundaries.

Flaming HRR methodology via thermopiles

Measuring flaming HRR via flue and chimney thermopiles

For an economical HRR apparatus, the oxygen consumption or even carbon dioxide production methodology as described in earlier sections may be avoided with thermopile HRR methodology. In the "Introduction" section, we briefly described modifying the MLC by adding a thermopile to the middle of the exhaust chimney. Here we justify that addition. Consider a control volume consisting of the sample holder, cone heater, and standard chimney attachment, rather than the control volume surrounding the flue gas only, as shown in Figure 10.

It is useful to start with a cone heater as a heat source that creates the natural buoyant air flow within and outside the chimney, and after that, the combustion of the fuel acts as an added heat source to motivate buoyant flue gas flow rate. Because the cone heater applies a constant heat flux to the sample, its heat production is constant, resulting in steady-state heat balance, given in the following equation

$$Q_{heater} = \dot{m}_{go}C_{ph}T_{ph} \quad \dot{m}_{go}C_{po}T_o + \int_0^{zp}(h_{conv}+h_{rad})(T_{ch} \quad T_0)2\pi Rdz \qquad (18)\leftarrow$$

The enthalpy rise rate, Q_{heater}, of the flue gases is given by the first two terms on the right side, and the flue gas heat losses to the sample, bench table, heater walls, and chimney via both radiant and convective heat are measured as heat losses from the control volume to the environment in the steady domain. T_c is the temperature of the chimney wall, T_p is the temperature of the plume air existing the stack, and T_0 is room temperature. Definition of other variables is provided in the nomenclature section. The subscript p refers to the plume gas, and the subscript c refers to the chimney wall. The subscript h refers to cone-heater-only condition, and the subscript g refers to plume gas combustion with cone heater. During fuel combustion, it may be assumed that all flaming heat release occurred within the control

volume. Because fuel combustion is generally unsteady, the heat balance of the control volume in the transient form will then require the flue gas heat losses to be also absorbed in the thermally thin barrier, as given in the following equation

$$Q_T + Q_{heater} = \dot{m}_g C_{pg} \quad T_p + \tau_p \dot{T}_p \qquad \dot{m}_{go} C_{po} T_o + \int_0^{z} \{\rho_c C_{pc} \delta \dot{T}_c + (h_c + h_r)(T_c \quad T_0 + \tau_c \dot{T}_c)\} 2\pi R dz \tag{19}$$

Note that deconvolutions of the gas thermopile signal, T_p, (with the time constant, τ_p) and chimney thermopile signal, T_c, (with the time constant, τ_c and representing the wall temperature, T_c) are now provided to capture the time response of the alternate measures of the flaming heat release, such as fuel mass rate times a constant flaming HOC, or the enhanced O_2 consumption or CO_2 production HRR methodology. This heat balance over the control volume differs from a similar analysis (Quintiere et al.)[11] in some significant features. In their modification of the MLC, they incorporated an insulation around the chimney, a nozzle on the top to measure the differential pressure for velocity measurement, and a gas probe for the oxygen content. Just as good or better accuracy with HRR via oxygen consumption can be obtained by merely placing the MLC under the cone calorimeter hood, or in our case, under the FPL's HRR instrumented hood. The use of insulation turns the chimney itself into a thermally thick material that is poorly modeled in the transient domain. The insulation delays further the needed cooling of the chimney walls to avoid heating the flue gas excessively when the combustion is extinguished.

Another sensible enthalpy rate approach used the relatively thicker aluminium plates surrounding the combustion source with thermocouples on both sides of the plate and measured the flue gas velocity with an anemometer (It is known as thermal canister, Anderson).[10] This is to measure temperature gradient and therefore obtain heat loss values via heat conduction approximation. However, the wall surface temperature gradient multiplied by its thermal conductivity is fundamentally equal to the convective and radiant heat losses to the environment whether in steady state or in transient mode, as modeled in equations (18) and (19). Because the combustion source is transient, the temperature profile is not linear across canister walls, causing the thermal canister method to be in error for the heat losses during this transient phase. Neither of these two approaches considered a deconvolution to the thermopile signal to improve response of the sensible enthalpy method, resulting in it being close to that of other HRR methods.

Moussan et al.[8] came up with a sensible HRR measure design by incorporating a water jacket around the combustion zone in which the temperature rise of the flowing water in the jacket was measured and the temperature rise and volume rate of the flue gas. This achieved very good steady-state estimations of the step-wise changes of the methane combustion HRR. There was a simple signal deconvolution of both water and flue gas HRR responses in the attempt to sharpen the predicted HRR profiles for the step changes in the methane flow rates. Assuming the exponential time response (which is a special case of the form shown in equation (19)), they obtained the needed time responses of 60 s, whereas the required time responses of the MLC flue gas thermopile are lower, varying between 5 and 120 s and averaging 55 s, while that of the MLC chimney steel wall with the thermopile affixed can have combined time constants varying between 70 and 150 s and averaging 125 s. Both time constants vary as functions of the flue gas thermopile temperatures because the convective and radiative coefficients are expected to vary under these conditions. An advantage of the water

jacket approach is that minimal empiricism is required because the water and flue gas flow rates are measured in addition to their temperature rises. Meanwhile, its design disadvantage is the low temperatures of the water jacket acting to quench partially the flaming, resulting in combustion that is more incomplete and higher radiant heat losses than would be the case in an open fire.

It therefore appears to be acceptable to leave the chimney in its original design and merely place thermocouples on the chimney surface to monitor the temperature difference between the thermally thin chimney walls and the environment. Then, the effective heat transfer coefficient that varies along the chimney height as multiplied by the local temperature difference and integrated along the whole chimney height provides the transient heat losses to the environment from the control volume, as described in the previous equation. Obviously, the rate of wall temperature rise can vary along the height of the chimney depending on the degree of combustion and radiant flux at a particular height. As a practical matter, the chimney thermopile is placed on the outside and halfway up the chimney, so that with the chimney wall temperature assumed to be varying at most as a linear function of height, the integrand for the heat losses can be treated as a constant when using wall temperature measured halfway up the chimney. With these simplifications, equation (19) minus equation (18) results in the solution for the flaming HRR, as in the following equation

$$\begin{aligned} Q_T = \dot{m}_g C_{pg} \quad & T_p + \tau_p \dot{T}_p \qquad \dot{m}_{gh} C_{pg} T_{ph} \quad + A_w (h_{conv} + h_{rad}) \\ & \{T_c + (\tau_c + \rho_c C_{pc} \delta / (h_{conv} + h_{rad})) \dot{T}_c \qquad T_{ch}\} \end{aligned} \tag{20}$$

The mass flow rate of the buoyancy-driven flue gas through the chimney can be given by the formula (Ong)[22]

$$\dot{m}_g = C_D \rho_{gp} \pi R^2 \sqrt{\frac{2 g z_p (T_p + \tau_p \dot{T}_p \quad T_0)}{T_0 \quad 1 + \frac{R^2}{R_0^2}}} \Bigg(\tag{21}$$

This mass flow rate of the flue gas formula differs slightly from a similar analysis (Quintiere et al.[11] or Anderson)[10] presumably because of the difference in the chimney design. The placement of the flue gas thermopile at the top of the chimney was then appropriate to implement equation (21), but the effect of the heat capacity of the thermocouples required a deconvolution of the thermopile signal with a time constant to obtain the true flue gas temperature at the top of the chimney. It is emphasized that by relying on the gas buoyancy to motivate the flue gas flow and external surface air flow, one can completely rely on the thermopiles to determine the combustion HRR via equation (20). Thus, in principle, there should be no need for added accessories, such as anemometers, pressure differential sensor, or oxygen concentration, if a good heat balance model is implemented.

Verification of flaming HRR via thermopiles

A two-step process was followed in our attempt to implement equations (20) and (21). The first step was to achieve an adequate deconvolution of the plume and chimney thermopile signals, whereas the second step was to determine the dominance of the derived temperatures of the plume versus the chimney on the HRR. It is conceivable that the chimney is long enough that most combustion heat is lost via the walls. We begin this process by showing

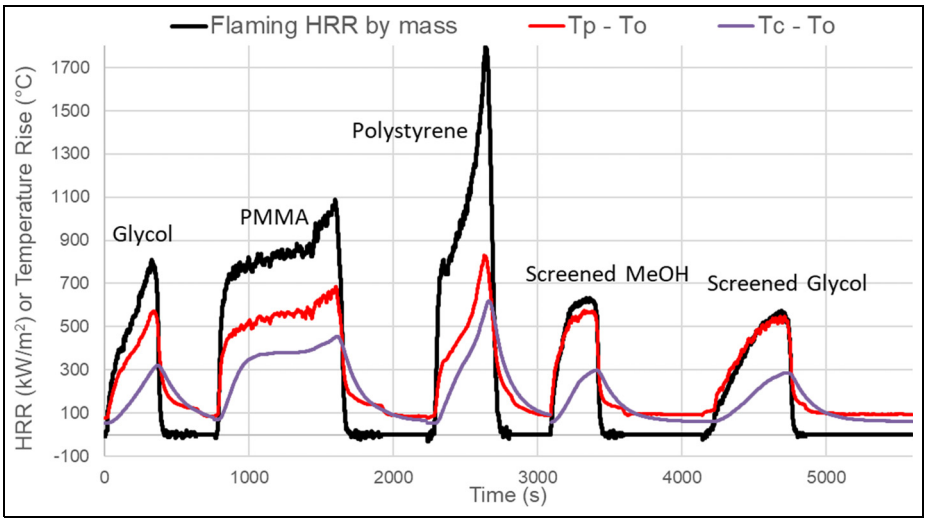

Figure 11. Temperature rises of the plume and chimney plotted alongside flaming HRR profiles.

the temperature rises of the plume and chimney for the four reference materials exposed to the irradiance of 50 kW/m^2 and the corresponding HRR = HOC × MLR in Figure 11 using the flaming HOC values listed in Table 1.

The plume gas temperature (T_p) may appear to have a rapid enough time response compared with the HRR responses, but then the difficulties start to arise. The peak plume temperatures for PS and PMMA seemed subdued compared with methanol and glycol, presumably the result of their higher radiant energy loss to the chimney walls from the higher production of soot. Hopefully, this additional radiant energy is reflected in the relatively higher chimney thermopile temperature (T_c), as appears to be true for the PMMA and PS fuel. After the fuel burns out, there is a rapid initial drop in plume gas temperatures, but this drop falters in reaching the equilibrium level because of the plume air being preheated by the still-hot sample holder and chimney walls. The plume gas temperature does another dip when the sample holder is removed to get ready for the next test. Therefore, the side effect of a more rapid plume gas temperature response is its increased sensitivity to the disturbances of the flow and heat releases, which could be difficult to compensate for. Conversely, the chimney thermopile temperatures appear to be slower responding in comparison, as expected, but are not affected by disturbances as much. In conjunction with the smoother temperature profile, the chimney thermopile temperature would be more suitable for deconvolution of its data.

The objective in the deconvolution of the plume and chimney thermopiles data is to create profiles that mimic the shapes of the HRR profiles obtained by HOC × MLR, which is shown as the black (highest) curve in Figure 12. Most importantly, the process is to derive a zero value when there is no combustion heat release. The next importance is to mimic the HRR profile shapes when the transient combustion is ensuing. This was achieved with equations (22) and (23)

$$T_{pd} = T_p \quad T_{ph} + \{p_1/(1 + p_2 T_p^{p_3})\}\dot{T}_p \qquad (22)\leftarrow$$

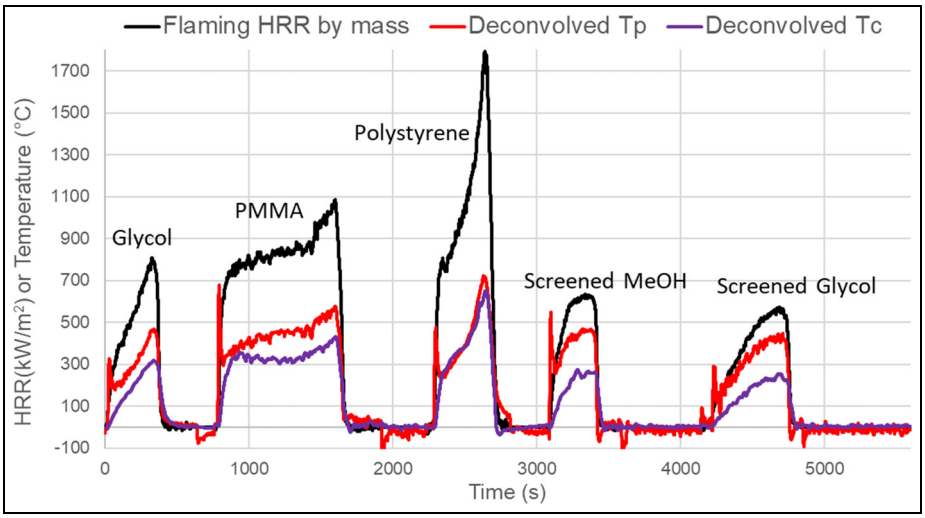

Figure 12. Deconvolution of plume and chimney thermopile signals and comparison with HRR.

$$T_{cd} = T_c \quad T_{ch} + \{c_1/(1 + c_2 T_p^{c_3})\}\dot{T}_c \tag{23}$$

where the subscript d refers to deconvolved calculated value. This required some empiricism for the time constants to be a function of the plume gas thermopile temperature, rather than constants. That is, both the plume and chimney thermopile data required minimal deconvolution at the peak HRR and maximal deconvolution in the valleys of the HRR profiles. The relatively higher noisiness in the deconvolved plume thermopile data in Figure 12 is reflected in its slopes despite efforts with the SG filters to smooth the noise, and disturbances such as removing the sample holder, which can result in spurious spikes. The dirtiness of the plume thermopile affected its response to the combustion heat by the time of the repeated burn of the glycol (the fifth test). Because of this, its holder was covered with a metal screen to reduce the irradiance to the liquid itself and extend the glycol burn time compared with the first glycol burn. All these difficulties noted with the plume gas thermopile are much less apparent with the deconvolved chimney thermopile data as shown in Figure 12. Indeed, the deconvolved chimney thermopile data seem promising on their own to fit the flaming HRR profiles for the four referenced materials simultaneously as shown in Figures 6 to 9 with the simple formula

$$Q_T = b_1 T_{cd} + b_2 T_{cd}^2 \tag{24}$$

And with the single set of coefficient values, $(b_1, b_2, c_1, c_2, c_3) =$ (23, 0.0072, 159.2, 0.000007281, 1.863) for all materials. These set of coefficient values are only applicable to the irradiance of 50 kW/m^2 and the chimney thermopile design. This formula retains only the second part of equation (20) pertaining to the heat losses to the chimney, with

$$\tau_c + \frac{\rho_c C_{pc} \delta}{h_{conv} + h_{rad}} \cong \{c_1/(1 + c_2 T_p^{c_3})\} \tag{25}$$

$$rA_w(h_{conv} + h_{rad}) \cong b_1 + b_2 T_{cd} \quad (26)\leftarrow$$

$$r = Q_T / A_w(h_{conv} + h_{rad}) T_{cd} \quad (27)\leftarrow$$

where r is an enhancement factor greater than unity accounting for flaming heat escaping with the flue gas. Apparently, the combustion heat losses to the chimney can act as a proxy for the sensible heat gain of the plume gases, given the difficulty of the plume gas thermopile for responding to the combustion heat and its sensitivity to conditioning and disturbances. Perhaps a better position for the gas plume thermopiles would be closer to the chimney walls to overcome various disturbances and reconsider equation (20).

A macro was created incorporating equations (23) and (24) and the resulting values of flaming HRR by thermopile smoothed with the exponential low-pass filter to reduce the noise level without much effect on the overall profile. It is noteworthy that this HRR measurement methodology has addressed the accuracy of the HRR zero level at ignition and at burnout as noted in our previous paper (Hasburgh et al.),[18] which is an advantage over other sensible heat release designs. The agreements with the flaming HRR from other methods are relatively good considering the problems with the standard methodology for the MLC. It is noted that the combustion of ethylene glycol and PMMA resulted in flames exceeding the chimney height at their peak HRR while that of the PS flame was mostly above the chimney height. Next, we turn to the low HRR measurement accuracy using the WPC materials, which resulted in low flame heights in the chimney, thus offering another challenge to the thermopile HRR measurement.

Verifying low HRR measures of WPC combustion

WPC board samples as reference material

The WPC boards were manufactured at the FPL. The base WPCs investigated consisted primarily of high-density polyethylene (HDPE) and wood flour (WF). The HDPE had a five melt flow index and was purchased from ExxonMobil (HD 6605.70, Houston, Texas). American Wood Fibers (Columbia, Maryland) supplied 40 mesh, mixed pine WF (AWF 4020). To maintain good composite surface characteristics, a lubricant was added to each composite. Struktol Company of America (Stow, Ohio) supplied the lubricant (TPW 113). In addition, two FRT systems typical for use in WPCs were investigated: (1) 3:1 ratio of decabromodiphenyl oxide (Saytex 102E, Albemarle Corporation, Baton Rouge, Louisiana) to antimony trioxide (BrightSun HB, China Antimony Chemicals Co., Ltd., Guangxi, China) and (2) ammonium polyphosphate (APP; Exolit AP 422, Clariant Corporation, Charlotte, North Carolina). WPCs without fire retardants had either 50% or 60% by weight WF, 5% lubricant, and the remainder HDPE. Composites with FRT incorporated 50% WF, 10% FRT, 5% lubricant, and the remainder HDPE. Accelerated weathering was applied to these WPC because exterior usage is a potential application of the product. More details are in a separate paper describing thermal degradation and fire performance of WPC.

Comparing flaming HRR measurements using WPC

To be assured of these HRR estimation methods for building products, the four different weathered WPCs were tested in the MLC under the HRR hood and with the cone calorimeter, especially if their HRR values were much lower than those of the reference materials

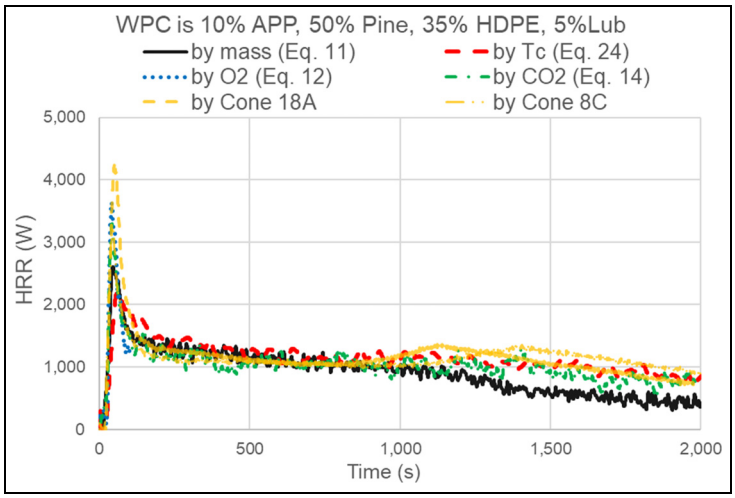

Figure 13. WPC with APP FRT (10% FRT/35% HDPE/5% Lub/50% Pine) as exposed to 50 kW/m^2 showing agreement among the various HRR calculations based on thermopile, oxygen consumption, and carbon dioxide production under the HRR hood and four different cone calorimeter tests.

and the PE (Stark et al.).[16] Their evaluation began with validating the flaming HRR of the thermopile method with that of the consumed oxygen method or the produced carbon dioxide method. However, during the tests with WPC, the oxygen analyzer malfunctioned partially for three cases, which meant that the carbon dioxide production became the reference flaming HRR values as calculated with equation (14). Where the flaming HRR by oxygen consumption method was functioning, it agreed with the flaming HRR by carbon dioxide production. The WPC fuel volatiles had the empirical formula, $C_6H_{11.2}O_4$, and the properties are listed in Tables 1 and 2. As a further verification to the flaming HRR calculations, some of the WPC tested also had the cone calorimeter counterparts of HRR measurements for this study with accelerated weathered samples and the earlier unexposed samples by Stark et al.[16]

Figure 13 shows the best example of the WPC with APP as the FRT, which also has the lowest HRR among the four WPCs tested. The low ~1 kW for most of the HRR profile is translated to 100 kW/m^2 of heat release flux, which is usually the borderline of the highest FRT-rated material. The initial peak HRR has the largest error margin, largely due to the differing time responses of the measuring methods. The higher noise level of HRR for both the instrumented hood and the MLC thermopiles compared with the cone calorimeter's HRR is to be expected, but the intent here was to compare the overall levels that agree quite well (within the seemingly 10% random error) among the various HRR measures, given the difficulties of calibrating near the zero HRR levels that are associated with treated materials. Because of the exponential low-pass digital filtering needed for both the instrumented hood and the MLC to reduce the noise level, their peak HRR was broadened somewhat as compared to that of the cone calorimeter test, which showed the higher and narrower HRR initial peaks.

Figure 14 shows the results with brominated FRT WPC (material described in detail by Stark et al.)[16] in which close agreement was obtained between the four cone calorimeter tests and HRR by the carbon dioxide production method. Although the HRR by the thermopile

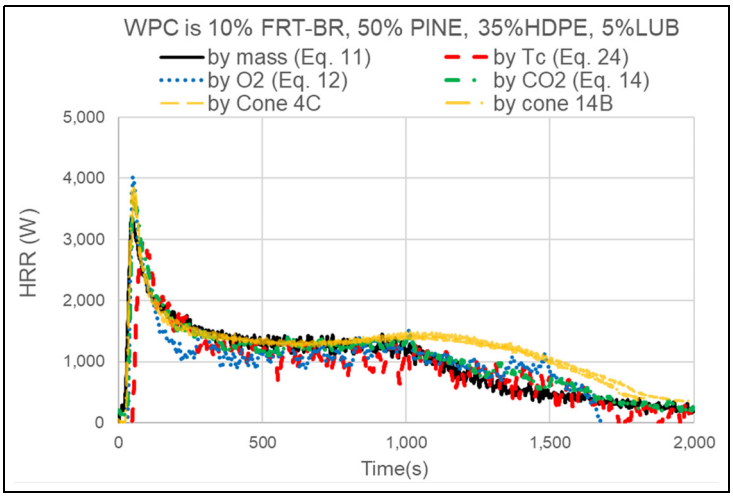

Figure 14. WPC with brominated FRT (10% FRT/35% HDPE/5% Lub/50% Pine) as exposed to 50 kW/m^2 showing agreement among the various HRR calculations based on thermopile, oxygen consumption, and carbon dioxide production under the HRR hood and four different cone calorimeter tests.

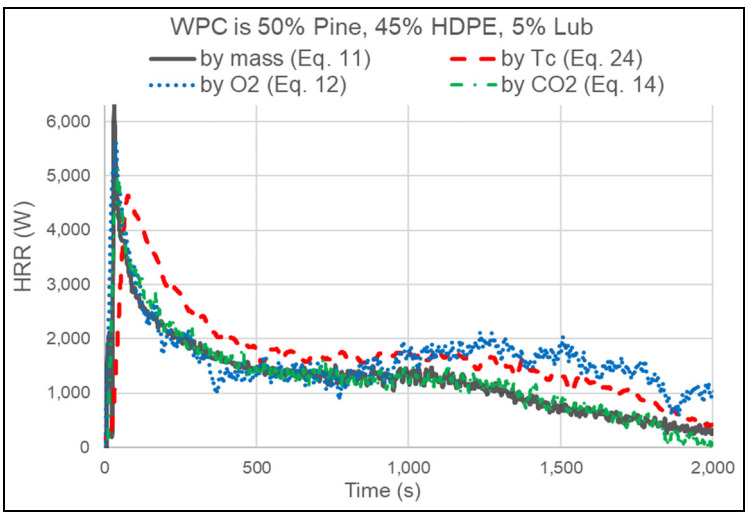

Figure 15. WPC (45% HDPE/5% Lub/50% Pine) as exposed to 50 kW/m^2 showing agreement among the various HRR calculations based on thermopile, oxygen consumption, and carbon dioxide production under the HRR hood.

method and the HRR by oxygen consumption are less in agreement with the other HRR methods, all tend to agree on a ~1.4 kW (or 140 kW/m^2) HRR plateau level for this WPC. For the untreated WPC, Figures 15 and 16 show also the ~1.4 kW HRR plateau level, indicating that the brominated FRT was relatively ineffective in reducing the HRR from that of untreated WPC, as was also found for unexposed samples (Stark et al.).[16] However, the APP

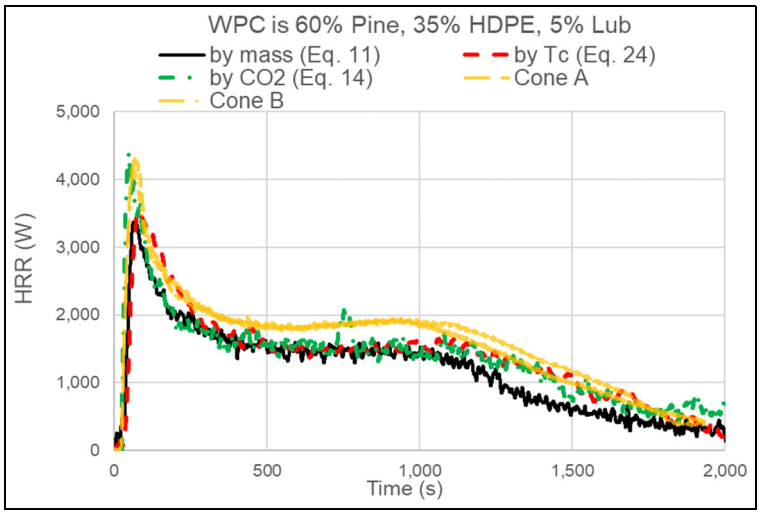

Figure 16. WPC (60% Pine/35% HDPE/5% Lub) as exposed to 50 kW/m^2 irradiance showing agreement among the various flaming HRR calculations based on thermopile, fuel mass loss, and carbon dioxide production under the HRR hood and two cone calorimeter tests.

Table 5. MLC flammability properties of the four WPC exposed to 50 kW/m^2 irradiances.

WPC material Percentage (and 5% Lub)	IT (s)	avgMLR (g/m^{2}s)	PHRR (kW/m^2)	THR (MJ/m^2)	HOCflm (kJ/g)
60% pine, 35% HDPE	NA	7.9	314	224	18.1
50% pine, 45% HDPE	25	8.0	430	288	22.0
10% BR, 50% pine, 35% HDPE	26	7.8	298	178	15.1
10% AP, 50% pine, 35% HDPE	31	5.7	218	185	18.2

Note: IT: ignition time; avgMLR: averaged mass loss rate; PHRR: peak heat release rate; THR: total heat release rate; HOCflm: overall flaming heat of combustion.

FRT could reduce the flaming HRR by 29% from that of the untreated WPC to possibly place it near a top-rated material. It is interesting that for all the WPCs, there was no indication of a large second peak HRR that is typical for wood materials.

Flammability assessment for four WPC with MLC

Indications are that the accelerated weathering has minimal effects on the HRR profiles, as shown in Figures 13 and 14 with cone calorimetry data of unexposed and weathered samples. This means the conclusions pertaining to flammability are like those of Stark et al.,[16] but the conclusions can now be based on the MLC observations as listed in Table 5. It is noted that the flammability related to ignition time and average fuel consumption rate is agreeable between the cone calorimeter measurements and the MLC measurements, as would be expected with similarity of design except for the differing HRR measurement methodologies. That is, the ignition time results are mixed, and the mass loss profile results

tend to follow that of the flaming HRR results, as shown in Figures 13 to 16, using the HOC of 18.6 kJ/g as an average value.

Conclusion

Various HRR methodologies were revisited in this article that were prompted by our investigation of the flammability of WPCs. There was a practical motivation to use the MLC for HRR determinations via the thermopile method. However, given the incomplete combustion nature of WPCs, which generated relatively higher amounts of CO and soot in diffusion flames, the flaming HOCs for various reference fuels required redetermination with the HRR hood calibrated for stoichiometric, flaming, and convective HRR of open fires of various sizes. Because the oxygen gas analyzer was inoperative part of the time, the HRR methodology based on CO_2 production was also upgraded to incorporate the correlation for stoichiometric HOC based on CO_2 mass produced and converted to flaming HOC due to CO and soot emissions. The result was the calculation of accurate flaming HOCs for the four reference materials that were used to calibrate both the instrumented HRR hood and the thermopile HRR methodology. Amendments to the various HRR standards should be sought, because computational fire modeling can benefit from better comparisons with the HRR data obtained. Obviously, improved statistical analysis associated with future interlaboratory studies would be beneficial.

MLC values of HRR via the new thermopile method were confirmed by oxygen consumption under the hood and with the cone calorimeter to apparently better than 10% error. The MLC thermopile method benefited from the use of a second thermopile located on the chimney to calibrate the coefficients to predict the flaming HRR from just the measurements with the air flue and chimney thermopiles, which proved adequate for the four standard reference materials. The application of this calibration is the prediction of flaming HRRs with time in the MLC for four different WPCs. They can be reported as HOCs by dividing them by the MLRs to provide another aspect to flammability measures. There was enough sensitivity in the MLC HRR to distinguish the various FRT of the WPC.

It is concluded that the upgraded sensible HRR methodology for the MLC has improved its ability to be used as a screening tool, although this is limited to the specified cone irradiance. However, results for other irradiance settings can be obtained using the improved flaming HOC methods presented here, which rely on low-cost reference materials, such as methanol, ethylene glycol, and PS. These methods provide a sensible HRR calibration on a much firmer basis than using the methane reference alone. The discussion of alternate sensible HRR designs reaffirmed the appropriateness of the MLC chimney design of a thin-walled steel vertical pipe with a thermopile attached at its midpoint.

Declaration of conflicting interests

The author(s) declared no potential conflicts of interest with respect to the research, authorship, and/or publication of this article.

Funding

The author(s) received no financial support for the research, authorship, and/or publication of this article.

ORCID iDs

Mark A Dietenberger https://orcid.org/0000-0002-8497-4149
Charles R Boardman https://orcid.org/0000-0002-9571-5601

References

1. Dietenberger MA and Boardman CR. HRR upgrade to mass loss calorimeter and modified Schlyter test for FR Wood. In: *Fire and materials conference*, San Francisco, CA, 28–30 January 2013, pp. 251–263. Madison, WI: USDA Forest Service, Forest Products Laboratory.
2. Dietenberger MA. Update for combustion properties of wood components. *Fire Mater* 2000; 26: 255–267.
3. Brohez S, Delvosalle C, Marlair G, et al. The measurement of heat release from oxygen consumption in sooty fires. *J* Fire Sci 2000; 18: 327–353.
4. Lonnermark A and Babrauskas V. *TOXFIRE—Fire characteristics and smoke gas analysis in under-ventilated large-scale combustion experiments* (Theoretical Background and Calculations (SP Report 1996:49). Boras: Swedish National Testing and Research Institute, 1999.
5. Babrauskas V.Heat of combustion and potential heat. In: Babrauskas V and Grayson SJ (eds) *Heat release in fires*. New York: Elsevier, 1992, pp. 207–223.
6. Tewarson A. Generation of heat and chemical compounds in fires. In: Tewarson A (ed.) *SFPE handbook of fire protection engineering* (3rd ed.) Boston, MA: Society of Fire Protection Engineers, 2002, pp. 82–161.
7. Dietenberger MA, Grexa O and White RH. *Reaction-to-fire of wood products and other building materials: part II, cone calorimeter tests and fire growth models* (Research Paper, FPL-RP-670). Madison, WI: USDA Forest Service, Forest Products Laboratory, 2012, p. 58.
8. Moussan F, Delfau JL, Vovelle C, et al. Heat release rate and effective heat of combustion measurements: a comparative study of thermal and oxygen consumption techniques. *J* Fire Sci 1995; 13: 482–499.
9. Filipczak R and Lyon RE. The correlation of heat release calorimetry measurements, DOT/FAA/AR-TN02/104, November 2002, https://www.tc.faa.gov/its/worldpac/techrpt/artn02-104.pdf
10. Anderson S. *Quantification of performance of wildfire chemicals using custom-built heat flux sensors*. MSc Thesis, University of Alberta, Edmonton, AB, Canada, 2015.
11. Quintiere JG, Lyon RE and Crowley S. A buoyancy-controlled bench scale fire calorimeter, fire testing session. In: *Interflam 2016*, Royal Holloway College, Nr Windsor, 4–6 July 2016.
12. ASTM E1321-12. Standard test method for determining material ignition and flame spread properties, 2013.
13. ASTM E906. Standard test method for heat and visible smoke release rates for materials and products using a thermopile method, 2006.
14. ASTM E2102-15. Standard test method for measurement of mass loss and ignitability for screening purposes using a conical radiant heater, 2015.
15. Grexa O, Dietenberger MA and White RH. *Reaction-to-fire of wood products and other building materials: part 1, room/corner test performance* (Research Paper, FPL-RP-663). Madison, WI: USDA Forest Service, Forest Products Laboratory, 2012, p. 51.
16. Stark NM, White RH, Mueller SA, et al. Evaluation of various fire retardants for use in wood flour/polyethylene composites. *Polym* Degrad Stab 2010; 95(9): 1903–1910.
17. ASTM E1354. Standard test method for heat and visible smoke release rates for materials and products using an oxygen consumption calorimeter, 2004.
18. Hasburgh LE, White RH, Dietenberger MA, et al. Comparison of the heat release rate from the mass loss calorimeter to the cone calorimeter for wood-based materials. In: *Proceedings of the fire and materials conference*, San Francisco, CA, 2–4 February 2015, pp. 116–126. New York: IEEE.
19. ASTM E2058-13A. Standard test methods for measurement of synthetic polymer materials flammability using a fire propagation apparatus (FPA), 2013.
20. Janssens ML. Methods and equations of fire calorimetry. In: *Special symposium on fire calorimetry* (eds Hirschler MM and Lyon RE), Gaithersburg, MD, 27–28 July 1995, pp. 11–22. New York: IEEE.
21. Janssens ML and Parker WJ.Oxygen consumption calorimetry. In: Babrauskas V and Grayson SJ (eds) *Heat release in fires*. New York: Elsevier, 1992, pp. 31–59.
22. Ong KS. A mathematical model of a solar chimney. *Renew Energ* 2003; 28: 1047–1060.

Appendix 1

Notations

a	ash mass fraction
b_i	fit coefficients in equation (23)
c_i	Fit coefficients in equation (22)
p_i	fit coefficients in equation (21)
c	carbon mass fraction
C	carbon symbol
C_d	drag coefficient in stack
C_p	heat capacity (kJ/g/K)
g	acceleration of gravity (m/s^2)

h	hydrogen mass fraction
h_c	convective heat transfer coefficient (kW/m^2/K)
h_r	radiative heat transfer coefficient (kW/m^2/K)
H	hydrogen symbol
Δh_f	heat of combustion (kJ/g)
k_{ext}	extinction coefficient (m^{-1})
$\dot{m}$	mass flow rate (g/s)
o	oxygen mass fraction
O	oxygen symbol
Q	heat release rate (kW)
R	radius of apparatus control volume (m)
r_oO	consumption mass/fuel mass
r_A	aromatic factor
s	sulfur mass fraction
S	sulfur symbol
T	absolute temperature (K)
T_c	absolute temperature (K) of chimney wall with thermopile
T_p	absolute temperature (K) of plume gases at chimney height
x	number of C atoms in monomer
y	number of H atoms in monomer
z	number of O atoms in monomer
z	height (m)
δ	chimney wall thickness (m)
ρ	density (kg/m^3)
τ	Time constant (s)

Author biographies

Mark A. Dietenberger, Ph.D. is a Senior Research General Engineer (Semiretired) in the Building and Fire Sciences work unit at the USDA Forest Products Laboratory. His research interests included (1) fire growth modeling coupled with experimentation, (2) WUI fire mitigation studies, including moisture dynamics, and (3) mechanistic studies of wood and vegetation degradation, including fire retardants.

Charles R. Boardman, is a General Engineer at the USDA Forest Products Laboratory.

Nicole Stark, PhD (she/her) is the Project Leader, Forest Biopolymer Science and Engineering work unit at the USDA Forest Products Laboratory.